

Alma Mater Studiorum Università di Bologna
Archivio istituzionale della ricerca

Biocompatible pectin-based hybrid hydrogels for tissue engineering applications

This is the final peer-reviewed author's accepted manuscript (postprint) of the following publication:

Published Version:

Tortorella S., Inzalaco G., Dapporto F., Maturi M., Sambri L., Vetri Buratti V., et al. (2021).
Biocompatible pectin-based hybrid hydrogels for tissue engineering applications. NEW JOURNAL OF
CHEMISTRY, 45, 22386-22395 [10.1039/d1nj04142h].

Availability:

This version is available at: <https://hdl.handle.net/11585/846102> since: 2022-01-18

Published:

DOI: <http://doi.org/10.1039/d1nj04142h>

Terms of use:

Some rights reserved. The terms and conditions for the reuse of this version of the manuscript are specified in the publishing policy. For all terms of use and more information see the publisher's website.

This item was downloaded from IRIS Università di Bologna (<https://cris.unibo.it/>).
When citing, please refer to the published version.

(Article begins on next page)

Biocompatible Pectin-based Hybrid Hydrogels for Tissue Engineering Applications

Silvia Tortorella^a, Giovanni Inzalaco^{b,c,d}, Francesca Dapporto^{b,c,d}, Mirko Maturi^a, Letizia Sambri^a, Veronica Vetri Buratti^a, Mario Chiariello^{b,c}, Mauro Comes Franchini^a and Erica Locatelli^{a*}

Hybrid hydrogels made of chemical modified pectin, gelatin and xanthan gum have been formulated and processed through a double crosslinking step, looking forward towards wound healing applications. The formulation of hybrid hydrogels finds its cornerstone in the possibility to create a supportive environment for cell adhesion and proliferation, ensuring the transport of nutrients via porous structures, together with mechanical properties closely comparable to the native tissue. The hydrogels present a good swelling behavior, resistance to dissolution and fragmentation in simulated biological environment (PBS1X and DMEM) for up to 20 days and the porous structure, as pictured via Scanning Electron Microscopy, has been foreseen to help cell migration and the exchange of biomolecules. Rheological characterization showed desired mechanical features, while the biocompatibility has been assessed via Live/Dead assay on murine fibroblasts. Finally, the hybrid hydrogels have also been proved suitable for mechanical extrusion, demonstrating the possibility of cell encapsulation in the future perspective of 3D bioprinting applications.

Introduction

Hydrogels, defined as high water-absorbing, chemically or physically bonded, insoluble and porous 3D networks, have gained significant interest in biomedical and in biomaterials research, as a result of their attractive characteristics. The appeal of hydrogels for various biomedical applications comes from their high water absorption capability (up to 99.9 wt%) and physicochemical characteristics that remind of many biological tissues.¹ Mechanical strength and degradation properties of hydrogels can be adjusted by modifying parameters such as the employed polymers (in terms of type and molecular weight), crosslinking agents, **porosity and synthesis conditions**.²⁻⁴ Consequently, these versatile properties allow hydrogels to be used for many biomedical applications, such as scaffolds for hard or soft tissues, carriers for cells and therapeutics, or as complete tissue substitutes.

Hydrogels can be divided into natural and synthetic according to the source of the material.⁵ In the last decades, the 'plastic free' trend has been increasingly focused on the use of natural hydrogels, the greatest part resulting from biological waste derivatives that are economically and quantitatively very attractive. As a consequence, naturally derived polymers, as proteins and polysaccharides, have been widely employed as

biomaterials for developing hydrogels which find many applications in the biomedical field, as, for example, in wound dressing, serving as tissue engineering scaffolds⁶, or drug delivery vehicles.⁷ Anyway, the majority of hydrogel formulations found in literature still employs synthetic polymers or synthetic/natural blends; in some cases the crosslinkers themselves are not biocompatible (e.g. glutaraldehyde⁸), or *hard* procedures for gelation are adopted (UV or X-ray exposure).⁹

Wound healing is a complex and dynamic process in which skin, and the underneath tissues, repair themselves after injury.^{10,11} Generally, a warm and moist environment promotes and boosts the healing. Severe wounds (injury or burning) affect the epithelium, but also the first layers of the skin endothelium.¹² In 2014 the annual cost for wound care was an average of \$2.8 billion. The projection for 2021 is expected to rise to \$3.5 billion. The 2018 market research report predicted that the global wound-closure products market would exceed \$15 billion by 2022.¹³

Over the last 30 years a large variety of biomaterials have been explored with the aim of finding novel solutions for such treatments. The range of natural materials available for this purpose is enormous: gelatin, pectin, starch, cellulose, alginate, chitin, collagen, hyaluronates, dextran - just to mention the best known.¹⁴ The chemical structure of these materials, primarily composed of sugar units and/or amino acid residues, are closely similar to protein, glycosaminoglycans and growth factor structures in the human body. Among these materials, pectin is one of the best candidates, mostly because it is a waste material produced from industrial manufacturing of fruit such as

^a Department of Industrial Chemistry "Toso Montanari", Viale Risorgimento 4, 40136, Bologna, Italy.

^b Istituto di Fisiologia Clinica (IFC), Consiglio Nazionale delle Ricerche (CNR), Siena, Italy

^c Core Research Laboratory (CRL), Istituto per lo Studio, la Prevenzione e la Rete Oncologica (ISPRO), Siena, Italy

^d Department of Medical Biotechnologies, University of Siena, Siena, Italy

oranges, apples, mango peels etc.¹⁵ Pectin structure is rich in galacturonic acid, meaning that it contains many carboxylic groups that, depending on the fruit source and the extraction method used, can be diversely esterified with methanol. Pectins are classified as high-methoxy (HM) and low-methoxy (LM) pectins, with more or less than 50% of all the galacturonic acid esterified. The esterification degree affects the gelation behaviour of pectin¹⁶: HM-pectins can form a gel under acidic conditions¹⁷ ($\text{pH} < 3.5$) together with high sugar concentrations¹⁸ ($> 55\%$); on the other hand LM-pectins form gels interacting with divalent cations (e.g. Ca^{2+} , Zn^{2+}), according to the idealized 'egg box' model, in which calcium ions and the negatively charged carboxyl groups of the galacturonic acid are combined together in ionic bridges.¹⁹ Since pectin is a naturally occurring polysaccharide containing carboxylic groups, it is expected to be used as a substitute for acrylic acid polymers, widespread candidates for wound dressing applications, without environmental problems.²⁰

Xanthan gum, as pectin, is a high molecular weight polysaccharide, with branched chains and acidic characteristics largely used as thickening agent in food, cosmetics and drilling fluids.²¹ Xanthan gum is mainly produced by *Xanthomonas campestris* in aerobic conditions from sugar cane, corn or their derivatives.²² Its structure is composed of D-glucosyl, D-mannosyl, and D-glucuronyl acid residues in a 2:2:1 molar ratio and variable proportions of O-acetyl and pyruvyl residues. Under low ionic strength or high temperature xanthan chains appear as disordered and flexible structures, whereas at low temperature or high ionic strength they present ordered structures (single or double helix conformations). At $\text{pH} > 4.5$ O-acetyl and pyruvyl residues are deprotonated, increasing charge density along the xanthan chains and enabling their physical crosslinking mediated by Ca^{2+} ions.^{23,24} The chemical structure of xanthan gum and pectin are depicted in **Figure 1**.

The capability of pectin and xanthan gum to easily crosslink and create single-component hydrogels, or multi-component hydrogels in combination with other materials, expands their use considerably in the field of regenerative medicine and wound healing. However, because of their polysaccharide structure, dedicated sites for cell adhesion, like, for example, the well-known RGD (Arginyl-Glycyl-aspartic acid) motif, are lacking.²⁵ This issue can be overcome by blending the chosen polysaccharides with other 'cell adhesive' materials, as, for example, gelatin. As a protein fragment derived by partial degradation of water-insoluble collagen fiber, gelatin has been largely used in the biomedical field, because of its attractive properties, including the biological origin, the biocompatibility / degradability with low antigenic impact, the gelling / thickening effect, and commercial availability at a relatively low cost.^{10,26,27} Gelatin is soluble in aqueous media and reversible gelation occurs at temperature ranges around 60°C ; therefore, gelatin-containing structures for long-term biomedical applications need to be crosslinked. Gelatin can easily be blended with pectin and xanthan gum to give spongy films, soft scaffold and hydrogels that can provide a promising environment for cellular adhesion and proliferation, together with a self-standing well cross-linked structure with desirable mechanical properties.²⁸

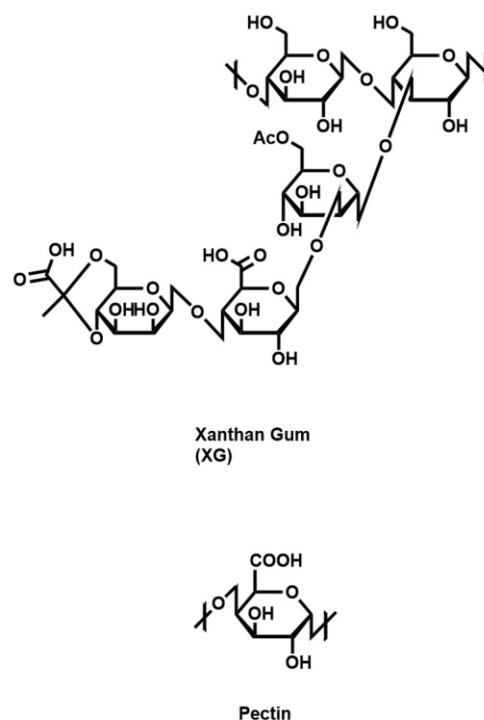


Figure 1. Xanthan Gum (XG) and Pectin chemical structures.

Glycerol and Chitin nanocrystals (CNC) addition can help the plasticisation and reinforce the mechanical structure of the hydrogel respectively. More in depth, to produce efficient scaffolds, the properties must be optimized, and plasticizers are often involved in this purpose. Small molecules such as polyols (sorbitol and glycerol) can intersperse and intercalate among and between polymer chains, disrupting hydrogen bonding and spreading the chains apart, for both enhancing flexibility, and water vapor or gas permeabilities.²⁹ On the other hand, nanochitin acts as the reinforcing phase, in order to fulfil the challenges related to weak mechanical properties: the reinforcement effect shown by nanocrystals is generally due to the formation of a percolating network of hydrogen bond.³⁰ In this work, the combination of pectin, gelatin and xanthan gum is expected to improve mechanical and biological properties of a wound dressing hydrogel. Moreover, it is not known in literature any hydrogel made by the combination of these three elements together, so far. Thus, we describe here a novel hybrid hydrogel formulation consisting of 100% natural and biocompatible polymers built *via* a double crosslinking mechanism: a chemical bonding between gelatin amino groups and pectin/xanthan gum carboxylic acid groups, and an ionic interaction of the latter with calcium ions. This work can act as the starting point for future formulations that can be tuned in terms of percentages for different aims and applications.

Materials and Methods

Reagents

Pectin (Poly-D-galacturonic acid methyl ester from apple, DE = 55.4%) was purchased from Merck Life Science. Calcium Chloride (anhydrous, 93%) and Glycerol (99.5+%) were purchased from Alfa Aesar. Xanthan Gum was purchased from TCI Chemicals. 1-ethyl-3-(3-dimethylaminopropyl) carbodiimide hydrochloride (EDC HCl) was obtained from Fluorochem, UK. Gelatin (type A, from porcine skin, BR-GEL 240, SSW) was obtained from Brace GMBH. Nanochitin was prepared by acid hydrolysis of chitin, which in turn is from Alfa Aesar. All the hydrogels intended for biological characterization and test were fabricated starting from sterile bulk materials and using sterilized glassware and consumables under a biosafety cabinet

Chemical Modification of Pectin

Firstly, to improve the capability of pectin of crosslinking with gelatine's amine groups, the degree of esterification (DE) of pectin is further reduced through an alkaline hydrolysis reaction (Figure 2). A proper amount of pectin is solubilized in ultrapure water under magnetic stirring; after the complete dissolution of the polysaccharide, a NaOH aqueous solution is added drop by drop (molar ratio pectin/NaOH equal 1:1 in the final volume). The reaction is kept under stirring, at 50 °C, until the solution becomes transparent and homogeneous. The purification is performed by dialysis against ultrapure water, checking the complete purification by measuring the waste-water pH. Then the product is freeze-dried (LIO5P 4K, 5Pascal, at 0.25 mmHg for 72 h). The powder obtained was characterized by FTIR and ¹H-NMR.

Synthesis of hybrid hydrogels

Modified-pectin is dispersed in ultrapure water (4% or 2% w/w, in the target hydrogel volume) at 37°C in a shaker. Each concentration, from now on, is intended as the concentration in the final hydrogel volume. Gelatin is added to reach a concentration of 2% w/w, the solution is heated to 45-50°C, to help gelatin dissolution. Xanthan gum powder is mixed to pectin+gelatin solution for a final concentration of 0.5% w/w. The complete formulation of final hydrogels is reported in Table 1. The mix is then poured into a Luer Lock syringe, taking care to eliminate bubbles. Separately an EDC solution 50 mM is prepared in ultrapure water and transferred into a second syringe. Through a female-female connector, the two syringes are coupled, and the polymers solution is mixed to the EDC solution by sliding the plunges from side to side. The hydrogel is now ready to be extruded; the second crosslinking step can be achieved by dipping the extruded/printed structure in a CaCl₂ 0.5 M solution for 10 min.

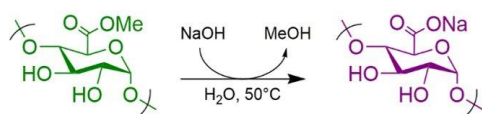


Figure 2. Pectin de-esterification scheme.

Characterization of Hydrogels

Macroscopically and qualitatively, the *vial tilt* method is used to confirm the sol-to-gel transition behaviour: after extrusion from the syringe into a glass vial, if the mixture does not flow when flipped over, it is reported as a gel (Table 1). The capability of being handled with a spatula or tweezers is an additional support to the fact that the hydrogel is self-standing.

Chemically modified Pectin is characterized using ATR-FTIR spectrometer (Cary 630 FTIR spectrometer, Agilent) operating in the region from 4000 to 600 cm⁻¹, resolution of 4 cm⁻¹. ¹H NMR spectra is obtained on a Varian Inova (14.09 T, 600 MHz) NMR spectrometer with pre-saturation solvent suppression sequence. In all recorded spectra, chemical shifts have been reported in ppm of frequency relative to the residual solvent peak (4.80 ppm for D₂O).

Swelling Tests. After being removed from the crosslinker solution, the hydrogel scaffolds are weighted and then incubated in PBS 1X solution (pH 7.4) or in DMEM at 37°C on an oscillating shaker. The samples' weights are measured again after 1, 2, 3, 4 and 7 days (T1, T2, T3, T4, T5) for any mass change due to swelling. Excess or free liquid from the scaffolds is accurately removed before weighing each sample. The swelling ratio of hydrogels is determined using the following equation:

$$\text{Swelling \%} = \frac{W_s - W_0}{W_0} \cdot 100$$

where W_s is the weight of the swollen hydrogels at specific time and W_0 is the early weight of the hydrogels at t_0 .

Degradation test. The hydrogels are freeze-dried after crosslinking and then their initial masses were measured. The samples are incubated in PBS 1X solution (pH 7.4) or in DMEM at 37°C on an oscillating shaker for 3, 7, 14 and 21 days to obtain the degraded scaffolds. The PBS or the DMEM solution is withdrawn and then the scaffolds are washed with deionized water two times, to remove salts. Finally, the samples are freeze-dried and weighed again. The hydrogel degradation is calculated using the following equation:

$$\text{Degradation \%} = \frac{W_0 - W_t}{W_0} \cdot 100$$

where W_t is the freeze-dried scaffold weight at specific time, and W_0 is the freeze-dried scaffold weight at the t_0 .

Gel	Pectin (wt.%)	Gelatin (wt.%)	Xanthan Gum (wt.%)	Chitin (wt.%)	Glycerol (vol%)	EDC (mM)	Tilt test
P1	1	1	0.5	0.25	1	50	X
P2	2	2					✓
P3	2	1					X
P4	4	2					✓

Table 1. Hydrogel formulations' content and related *vial tilt* test outcome: P2 and P4 have been selected for following experiments due to their successful gelation.

Mechanical characterization. Rheological experiments were performed on an Anton-Parr MCR102 modular compact rheometer with a DPP25-SN0 geometry, meaning a double plate geometry with a diameter of 25 mm. Amplitude sweep measurements were performed at 25°C at a frequency of 5 rad s⁻¹, with sample strains ranging from 0.1% to 1000%. Dynamic-mechanical thermoanalysis (DMTA) was carried out in the +4/+40°C temperature range with a constant heating rate of 2.5°C/min at a constant strain of 0.5%, while keeping the angular frequency at 5 rad s⁻¹. Rotational viscosity experiments (controlled shear rate tests, CSR) were performed at 37°C by varying the shear rate from 0.1 to 1000 s⁻¹.

Determination of porosity. The freeze-dried hydrogels were observed with a Zeiss EVO LS LaB6 scanning electron microscope (SEM), operated at 5 kV. Prior to examination, the hydrogels were sputter coated with gold. The average pore size of hydrogels was determined from micrographs using 10 randomly measured pores.

Cell Experiments to determine Hydrogels Cytotoxicity: Live/Dead Assay

NIH3T3 cells (5 × 10⁴) were seeded on polystyrene 24-wells culture plates, and incubated with hydrogel obtained after the crosslinking of 400 µl of pre-hydrogel, in order to test its intrinsic cytotoxicity. A minimum of three samples and a control well without hydrogel were studied. Treated cells and control samples were incubated at 37°C, 5% CO₂ for 48h. Cell

viability was assessed using Live/Dead Double Staining Kit (Sigma-Aldrich). Dual fluorescent staining solution Cyto-Dye and Propidium Iodide was added to each well according to manufactory protocols. The kit utilizes Cyto-dye, a permeable green fluorescent dye, to stain live cells, and propidium iodide, a non-permeable red fluorescent dye that can only enter the cells when their membrane is damaged (dead cells). The images were acquired by fluorescent microscope Leica DMI3000 B.

Statistical analysis. All quantitative data were expressed as the mean and standard deviation. One sample for each formulation (in the pre-gel and the crosslinked form) was used for rheology characterization, and three samples for degradation and cell viability assay. Cells count was performed using Volocity software and data were analyzed using GraphPad Prism 6.

Results

Hydrogel Features

The hybrid hydrogel synthesis was performed using a double cross-linking strategy: the first one by employing EDC chemistry, while the second one by exploiting the ionic interaction with CaCl₂. The reaction is depicted in **Figure 3**. Such double crosslinking approach was selected to combine the mechanical resistance and chemical stability conferred by the covalent connections with the flexibility and reversibility of ionic interactions, as already observed for other polysaccharides.^{31,32}

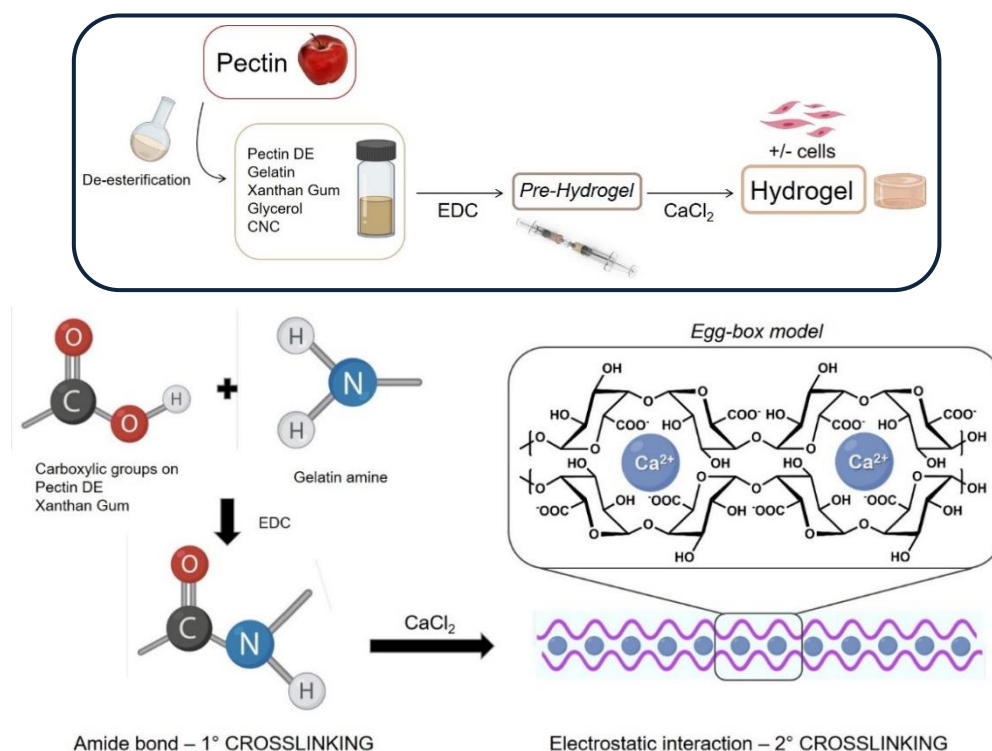


Figure 3. Schematic representation of chemical and ionic interactions occurring in the hydrogel synthesis. a) Hydrogel synthesis workflow. b) EDC chemistry for covalent amidic bond formation. c) Ionic cross linking with Ca cations ('egg box' model).

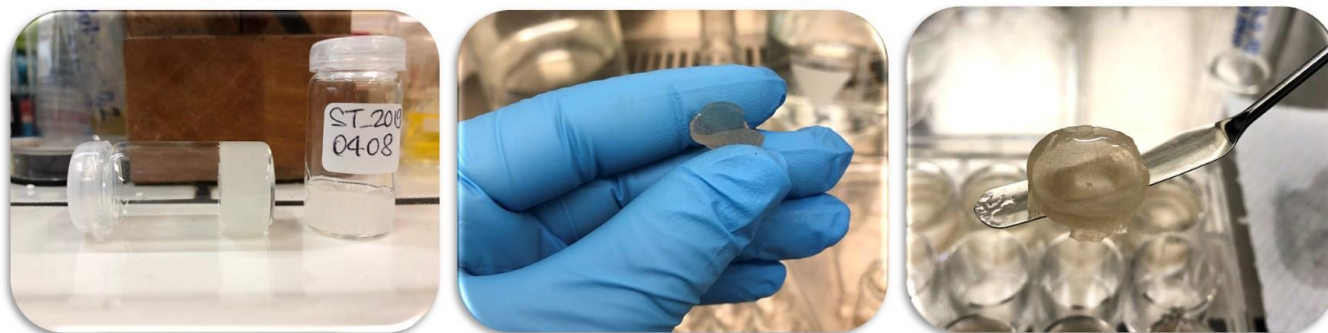


Figure 4. Macroscopic aspect of the hybrid hydrogel.

The occurred gelation was macroscopically verified by tilting the vial and observing the gel not flowing but standing still. The moulded structure is easy to handle and manipulate with a spatula or tweezers; the hydrogel looks bendy and transparent (Figure 4).

FTIR analysis together with $^1\text{H-NMR}$ (Figure 5) confirmed the complete de-esterification of Pectin. The strong band at 3400 cm^{-1} is assigned to the ν (O–H) stretching vibrations of hydrogen-bonded and free hydroxyl groups. The band at 2940 cm^{-1} is attributed to ν (C–H) stretching of CH_2 groups [24]. The region from 1800 to 1500 cm^{-1} is particularly useful to define the esterification degree. In this regard the peak around 1740 cm^{-1} is the C=O stretch observed in the ester deriving from acetyl group (COCH_3). The peak at 1630 cm^{-1} is related to the -OH tensile vibration band, deriving from carboxylic groups (COOH). As we can easily see from the two overlapped spectra, the C=O peak quite noticeable in the native Pectin from apple,

almost disappeared in de-esterified Pectin, fully replaced by the peak at 1630 cm^{-1} . In addition the peaks around 1400 cm^{-1} and 1250 cm^{-1} respectively represent the C–O–H in the bending vibration and the asymmetric C–O–C tensile vibration, directly related to the abundance of –O– CH_3 (methoxyl) groups. Finally the strong peaks at 1100 cm^{-1} and 1020 cm^{-1} are the symmetric C–O–C tensile vibration. $^1\text{H-NMR}$ reinforces this evidence, showing the $-\text{CH}_3$ peak disappearing at 4.05 ppm after de-esterification of pectin.

The swelling properties of scaffolds define the ability of nutrients to be exchanged between the environment and cells in order to regenerate a new tissue. The capability of being hydrated is strongly connected to swelling efficiency, which determines also the hydrogel solidity inside the biological systems.³³ The swelling behaviour of the hybrid hydrogels in PBS/DMEM is depicted in the graph in Figure 6. The samples in this study were incubated in PBS 1X or DMEM to evaluate the rate of water absorption over time. The swelling test results show a coherent trend for the two different hydrogel formulations, with reference to the solution wherein they are dipped. For what concerns gel P2, a small first increase both in PBS (5%) and in DMEM (1%) is observed, followed by a higher

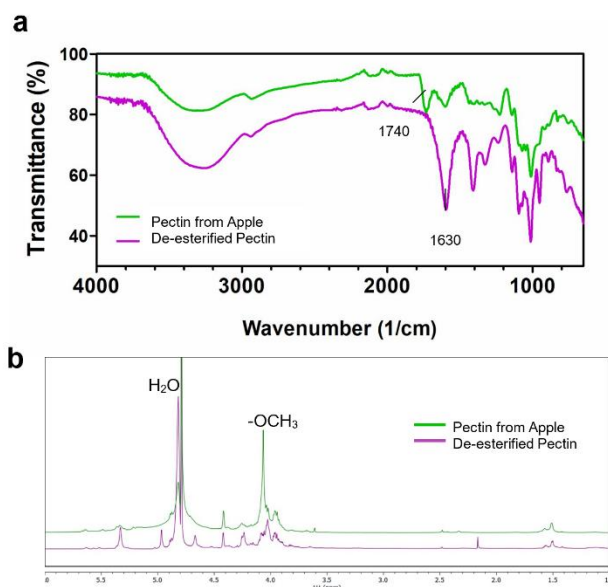


Figure 5. Native Pectin from Apple vs de-esterified Pectin characterization: a) FTIR spectra showing ester (1740 cm^{-1}) and carboxylic group (1630 cm^{-1}) peaks' trend; b) $^1\text{H-NMR}$ (600 MHz, D_2O 10%) spectra showing $-\text{OCH}_3$ disappearing at 4.05 ppm after de-esterification of pectin.

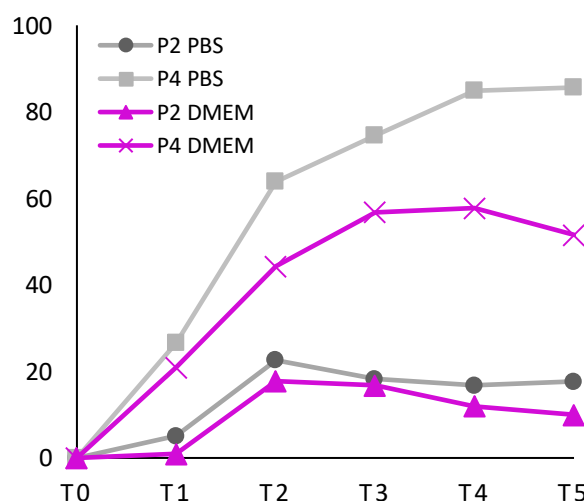


Figure 6. The absorption rate of the samples in different solution (PBS grey lines, DMEM pink lines) is indicated by the change in mass of the samples over time (T1 = 1 day, T2 = 2 days, T3 = 3 days, T4 = 4 days, T5 = 7 days).

swelling after 48 h (up until 20% ca). After 72 h, the hydrogel in PBS reaches a *plateau* that will be kept until the end of the test; on the other hand, the scaffold in DMEM starts losing mass after 96h, probably due to the degradation/fragmentation process starting. The difference that we observed for the two solutions in guiding the swelling behaviour is coherently found in P4 samples: they show a 20% increase in swelling ratio after 24 h (in turn, 20.9% of the mass for DMEM samples and 26.6% for PBS samples). The trend keeps growing after 48 and 72 h reaching a maximum of 85% and 57.7% for PBS and DMEM respectively. Consistently with the P2 trend, but 24 h later, the P4 reaches a *plateau* if it is dipped in PBS, while starts its degradation in DMEM. The difference in the formulation can easily lead and influence the scaffold's water absorption rate. The higher Pectin content in P4 hydrogels (4%) compared with the lower in P2 hydrogels (2%) can realistically be the reason why we found two swelling rates so quantitatively dissimilar, but coherent in the curve trend. PBS and DMEM also differently affect the swelling of the scaffolds, as observed in the different outcomes of the curves.

The degradation of hydrogels was also studied: both in PBS1X and in DMEM at 37°C, all the scaffolds are resistant to degradation/fragmentation and single components' dissolution for up to 21 days, with a residual mass of >99.8% for both the formulations.

The freeze-dried hydrogel shows a porous structure as imaged via SEM (**Figure 7**). The average pores dimension was in the range of 5-25 μm . The porous structure is crucial for

	$\gamma_L^{(a)}$ (%)	$G'_L^{(b)}$ (kPa)	$G''_L^{(b)}$ (kPa)	$\tau_{(y)}^{(c)}$ (Pa)	$\tau_{(f)}^{(d)}$ (Pa)
P2 (pregel)	4.6	0.19	0.017	8.9	190
P2 (crosslinked)	1.0	17	3.2	170	400
P4 (pregel)	10	0.14	0.012	9.2	225
P4 (crosslinked)	0.31	65	14	205	490

(a) Strain at the limit of the linear viscoelastic (LVE) range

(b) Storage and loss moduli in the LVE range

(c) Yield stress

(d) Flow stress

Table 2. Quantification of the main rheological parameters obtained by amplitude sweep measurements at 25°C.

guaranteeing the growth and migration of cells, the oxygen permeability and the delivery of potential small molecules encapsulated into the hydrogel or from/to the cell themselves. The viscoelastic properties of the prepared hydrogels are firstly evaluated by exploiting amplitude sweep measurements, comparing the behaviour of hydrogels P2 and P4 before and after the ionic crosslinking. The obtained diagrams of storage and loss moduli (G' and G'' , respectively) plotted against the extent of deformation and against the measured shear stress are shown in **Figure 8**. From the amplitude sweep measurements, it is possible to quantify the mechanical performances of the hydrogels before and after crosslinking, and the corresponding numerical value are collected in **Table 2**.

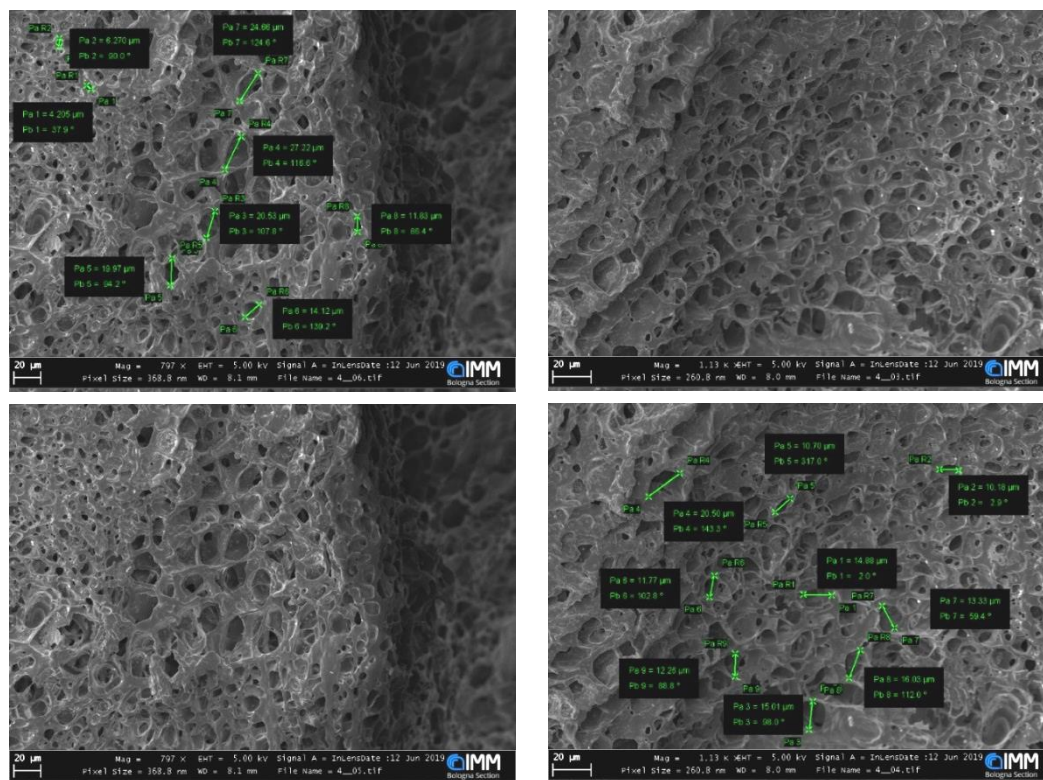


Figure 7. Hybrid Hydrogel SEM microscopy. Both formulations (P2 left, P4 right) show the same porous structure.

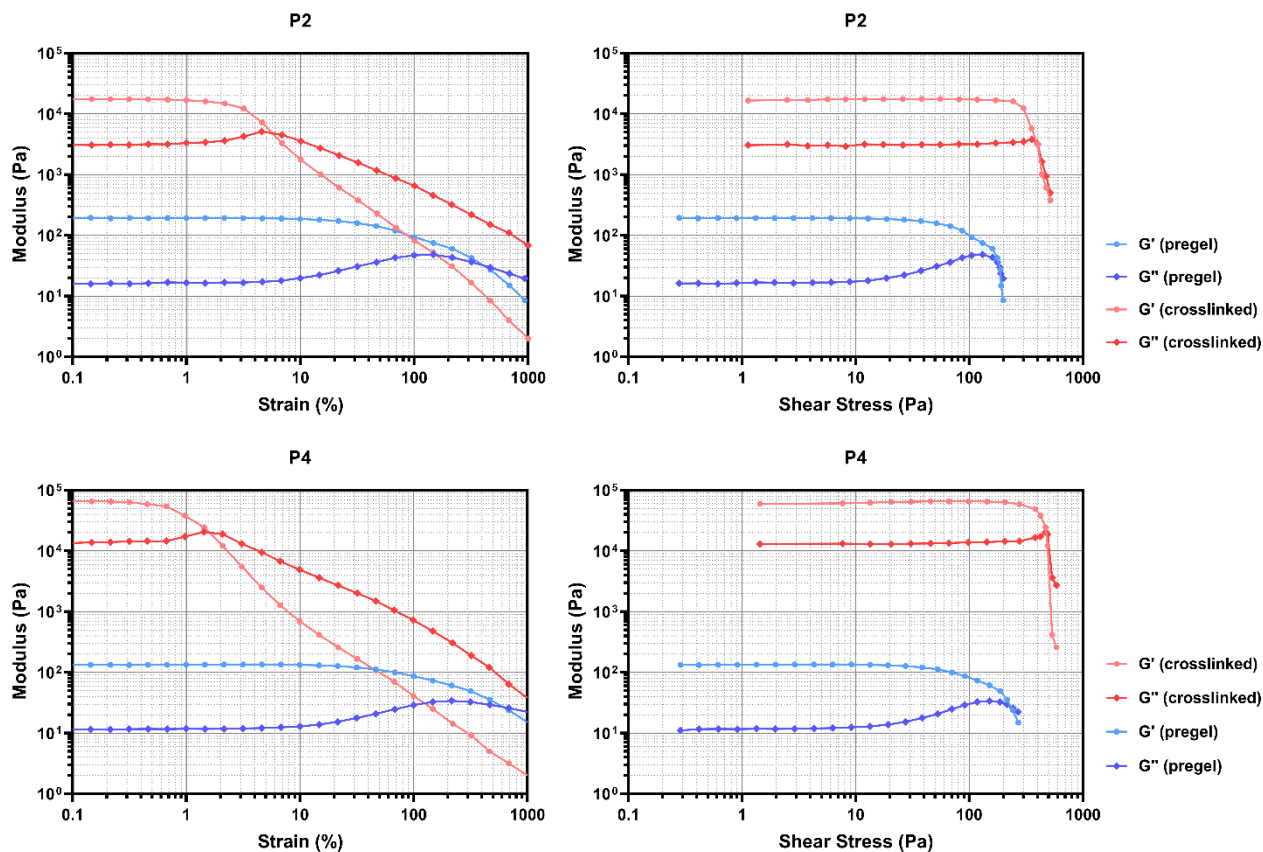


Figure 8. Amplitude sweep measurements on P2 (top) and P4 (bottom) hydrogel before (blue gradient) and after (red gradient) crosslinking with Ca^{2+} ions, plotted against the extent of deformation (left) or the measured shear stress (right).

From this data it is possible to conclude that an increase in the amount of pectin in the hydrogel formulations reflects in an extension of the linear viscoelastic (LVE) range, while both storage and loss moduli get slightly smaller. On the other hand, the rheological features of crosslinked gels are much more strongly affected by the amount of pectin, and this is expected due to the fact that Ca^{2+} ions mostly interact with free carboxylic groups on pectin. The crosslinked gels, in fact, display storage

moduli in the order of tens of kPa, and the lower values obtained for LVE range limits together with the increased yield and flow stresses when compared to non-crosslinked pre-gels reveal that both P2 and P4 crosslinked hydrogels display the stiffness and the toughness required for wound healing on-skin applications.³⁴ Then, dynamic-mechanical thermoanalysis (DMTA) was performed by fixing the strain of the sample at 0.5% and measuring the storage and loss moduli at different temperatures ranging from $+4^\circ\text{C}$ to $+40^\circ\text{C}$ (Figure 9).

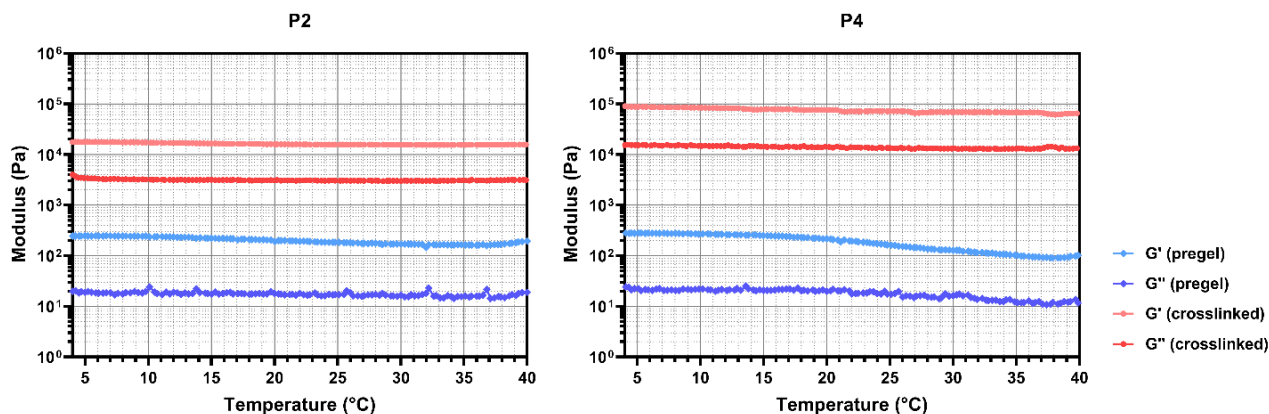


Figure 9. Dynamic-mechanical thermoanalysis (DMTA) of P2 (left) and P4 (right) hydrogel samples before (blue gradient) and after (red gradient) crosslinking with Ca^{2+} ions.

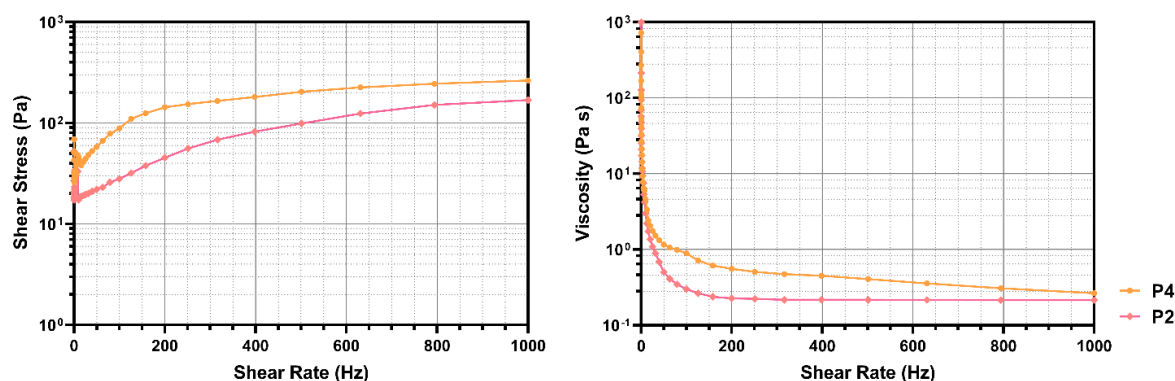


Figure 10. Rotational viscosity at controlled shear rate (CSR) tests performed on P2 and P4 pregels.

The analysis reveals a slight reduction in the storage modulus of pre-gels by increasing temperature, while the crosslinked gels have demonstrated structural and mechanical stability over all the explored temperature range. Finally, the extrudability and printability of pectin-based non-crosslinked hydrogels was evaluated by rotational viscosity experiments (Figure 10), which confirmed the shear-thinning behaviour of such formulations. In fact, even though they display high viscosity at rest, it drops below 1 Pa s after the application of relatively small rotational stresses (around 50 Hz).

Cytotoxicity

The hydrogel scaffolds are formulated in order to be employed in tissue engineering; thus, it is essential to assess their cytotoxicity and biocompatibility.

NIH3T3 viability has been assessed by Live/Dead assay on 5×10^4 cells seeded on 24-well plates wherein the hydrogels were dipped after crosslinking and a rapid wash in PBS. The L/D assay shows no toxicity after 48 h culture (Figure 11 bottom), displaying rising growth and proliferation, as previously confirmed by optical microscopy monitoring during the incubation period (Figure 11 top).

Discussion

In the field of tissue engineering, and in particular wound healing, a suitable hydrogel is expected to offer a good not cytotoxic environment for cell viability, allowing chemicals' exchange to cross its structure, and show properties that closely resemble the native tissue. The extracellular matrix (ECM) of skin is composed of a variety of polysaccharides, water and collagen proteins which give the skin remarkable properties.³⁵ The elasticity and compressibility of this tissue are due to the combination of two main classes of ECM molecules, which are secreted by fibroblasts and epidermal cells. These are: 1) Fibrous structural proteins, (as collagens, elastin and laminin) which give the ECM strength and resilience and 2) Proteoglycans, such as dermatan sulfate and hyaluronan, typically consist of multiple glycosaminoglycan chains (made from repeating disaccharide units) that branch from a linear protein core. The presence of polysaccharides with a strong

hydrophilic behavior is therefore important in smart hydrogel formulations: these components are highly negatively charged and thus attract osmotically Na^+ , resulting in large amounts of water retained into their matrix. These molecules tend to occupy a huge volume relative to their mass, giving gels at very low concentrations. The hydrophilic nature also provides swelling pressure (turgor) which enables the gels to resist to compression forces. Integration of collagen, or proteins (e.g. gelatin) derived from collagen, is critical for the success of hydrogels in skin regeneration. Putting together these requirements, pectin-based hybrid hydrogels are formulated, by modifying pectin chemical structure as needed. This modified-pectin is able to generate hydrogels in a divalent cations-rich environment, while the prior chemical crosslinking EDC chemistry helps stabilizing the amide linkage between the carboxylic-rich (pectin-xanthan gum) and the amine-rich (gelatin) portions. The resulted matrix is moreover reinforced by nanochitin homogeneously distributed inside the network. Abovementioned interactions and chemical bonds significantly rise the mechanical properties of hydrogels that are most expected to meet the requirements for skin regeneration aims. Previous works on hybrid materials made of pectin and/or gelatin used high amounts of ingredients, physical crosslinking, cytotoxic chemicals or long and multi-step chemical reactions.^{9,36,37} We can say that our hybrid pectin-based hydrogels, thanks to the specific modification of pectin and to the double crosslinking, are easy to produce and handle, completely bio-based and low-cost. Moreover, the pre-gel we developed allows easy extrusion and is 100% made in water, avoiding use of any organic solvent, (e.g. Chloroform, DMSO), hazardous (e.g. glutaraldehyde) or expensive (e.g. genipin) reagents, making it very promising for 3D bioprinting purposes. The rheological characterization in terms of storage and loss moduli calculation reveals that stiffness and strength of pectin hydrogels fully match with the native skin and soft tissue in general (1 to 100 kPa).³⁸

The pectin-based hydrogel precursor easily forms gel *in-situ* and, thanks to the porous structure, can act as a 3D matrix to allow nutrients and oxygen exchange. These hybrid hydrogels will be soon subject of further studies in ECM protein secretion, gene expression and differentiation of encapsulated stem cells, and studies with animal models.

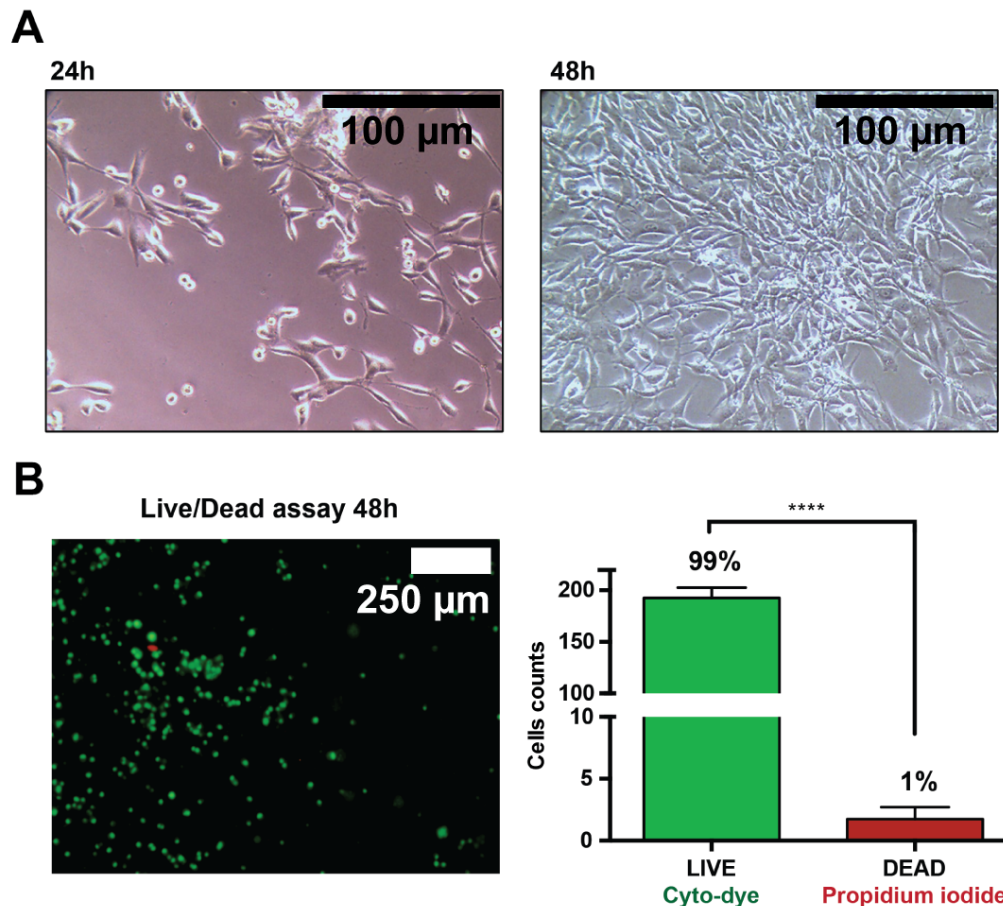


Figure 11. A) Optical micrographs of NIH3T3 cells seeded 24 and 48 hrs in presence of Pectin Hydrogels. B) Fluorescence merged images of Live/Dead assay of NIH3T3 cells seeded 48 hrs in presence of Pectin hydrogels (left panel). Cells were counted using Volocity software (right panel).

Conclusions

The synthesis of pectin-based hybrid hydrogels involving EDC chemistry and subsequent ionic crosslinking of Ca^{++} ions and carboxylic groups on polysaccharides is here reported. Each ingredient of the formulation has been chosen for a specific reason, resembling the ECM background: in particular, pectin is the core character, the polysaccharide part that gives the main structure to the scaffold, providing turgor and swelling performances. On the other hand, gelatin mimics the collagen counterpart and, together with pectin, forms the stable amide bonds for the formation of the gel. The hybrid hydrogels were characterized by desirable pore diameter and swelling behavior for molecules and oxygen exchange with tissue and cells. The use of hydrophobic nanochitin in the formulation increased crystallinity and stability against dissolution in aqueous media. Every ingredient of the hybrid hydrogels is 100% biocompatible and does not display cytotoxicity. The pectin-based hydrogels are potentially cost-effective for future cell encapsulation and delivery of nutrients and growth factors for wound healing applications.

Author Contributions

Conceptualization: E.L., M.C.F.
 Data curation: S.T., G. I.,
 Formal analysis: M.M., E.L., V.V.B.
 Funding acquisition: M.C.F., M.C.
 Investigation: S.T., F.D., G.I.
 Methodology: M.M., E.L., V.V.B.
 Supervision: M.C.F., M.C., L.S.
 Writing – original draft: S.T.
 Writing – review and editing: M.M., L.S., E.L.

Conflicts of interest

There are no conflicts to declare.

Acknowledgements

The University of Bologna is gratefully acknowledged.

Notes and references

- 1 B. Ozcelik, in *Biosynthetic Polymers for Medical Applications*, Elsevier, 2016, pp. 173–188.
- 2 A. Deng, Y. Yang and S. Du, *Appl. Sci.*, 2021, **11**, 5096.
- 3 A. Samourides, L. Browning, V. Hearnden and B. Chen, *Mater. Sci. Eng. C*, 2020, **108**, 110384.
- 4 M. J. Gupte, W. B. Swanson, J. Hu, X. Jin, H. Ma, Z. Zhang, Z. Liu, K. Feng, G. Feng, G. Xiao, N. Hatch, Y. Mishina and P. X. Ma, *Acta Biomater.*, 2018, **82**, 1–11.
- 5 T. Zhu, J. Mao, Y. Cheng, H. Liu, L. Lv, M. Ge, S. Li, J. Huang, Z. Chen, H. Li, L. Yang and Y. Lai, *Adv. Mater. Interfaces*, 2019, **6**, 1–22.
- 6 S. Mantha, S. Pillai, P. Khayambashi, A. Upadhyay, Y. Zhang, O. Tao, H. M. Pham and S. D. Tran, *Materials (Basel)*, 2019, **12**, 3323.
- 7 J. Li and D. J. Mooney, *Nat. Rev. Mater.*, 2016, **1**, 16071.
- 8 S. Cui, B. Yao, M. Gao, X. Sun, D. Gou, J. Hu, Y. Zhou and Y. Liu, *Carbohydr. Polym.*, 2017, **157**, 766–774.
- 9 R. F. Pereira, A. Sousa, C. C. Barrias, P. J. Bártolo and P. L. Granja, *Mater. Horizons*, 2018, **5**, 1100–1111.
- 10 H. U. Zaman, J. M. M. Islam, M. A. Khan and R. A. Khan, *J. Mech. Behav. Biomed. Mater.*, 2011, **4**, 1369–1375.
- 11 H. N. Wilkinson and M. J. Hardman, *Open Biol.*, 2020, **10**, 200223.
- 12 W.-K. Loke, S.-K. Lau, L. L. Yong, E. Khor and C. K. Sum, *J. Biomed. Mater. Res.*, 2000, **53**, 8–17.
- 13 C. K. Sen, *Adv. Wound Care*, 2019, **8**, 39–48.
- 14 A. Bianchera, O. Catanzano, J. Boateng and L. Elviri, in *Therapeutic Dressings and Wound Healing Applications*, Wiley, 2020, pp. 337–366.
- 15 S. Thakur, J. Chaudhary, V. Kumar and V. K. Thakur, *J. Environ. Manage.*, 2019, **238**, 210–223.
- 16 D. Gawkowska, J. Cybulska and A. Zdunek, *Polymers (Basel)*, , DOI:10.3390/polym10070762.
- 17 F. Voragen, H. Schols and R. Visser, Eds., *Advances in Pectin and Pectinase Research*, Springer Netherlands, Dordrecht, 2003.
- 18 H. Kastner, U. Einhorn-Stoll and B. Senge, *Food Hydrocoll.*, 2012, **27**, 42–49.
- 19 D. E. Ngouémazong, F. F. Tengweh, I. Fraeye, T. Duvetter, R. Cardinaels, A. Van Loey, P. Moldenaers and M. Hendrickx, *Food Hydrocoll.*, 2012, **26**, 89–98.
- 20 H. Mert, B. Özkahraman and H. Damar, *J. Drug Deliv. Sci. Technol.*, 2020, **60**, 101962.
- 21 V. B. Bueno, R. Bentini, L. H. Catalani and D. F. S. Petri, *Carbohydr. Polym.*, 2013, **92**, 1091–1099.
- 22 R. E. Edens, *J. Am. Chem. Soc.*, 2005, **127**, 10119–10119.
- 23 D. Bergmann, G. Furth and C. Mayer, *Int. J. Biol. Macromol.*, 2008, **43**, 245–251.
- 24 A. F. Dário, L. M. A. Hortêncio, M. R. Sierakowski, J. C. Q. Neto and D. F. S. Petri, *Carbohydr. Polym.*, 2011, **84**, 669–676.
- 25 S. E. D'Souza, M. H. Ginsberg and E. F. Plow, *Trends Biochem. Sci.*, 1991, **16**, 246–250.
- 26 M. C. Gómez-Guillén, B. Giménez, M. E. López-Caballero and M. P. Montero, *Food Hydrocoll.*, 2011, **25**, 1813–1827.
- 27 M. C. Echave, L. S. Burgo, J. L. Pedraz and G. Orive, *Curr. Pharm. Des.*, , DOI:10.2174/0929867324666170511123101.
- 28 N. Davidenko, C. F. Schuster, D. V. Bax, R. W. Farndale, S. Hamaia, S. M. Best and R. E. Cameron, *J. Mater. Sci. Mater. Med.*, 2016, **27**, 148.
- 29 L. Ballesteros-Mártinez, C. Pérez-Cervera and R. Andrade-Pizarro, *NFS J.*, 2020, **20**, 1–9.
- 30 B. Joseph, R. Mavelil Sam, P. Balakrishnan, H. J. Maria, S. Gopi, T. Volova, S. C. M. Fernandes and S. Thomas, *Polymers (Basel)*, 2020, **12**, 1664.
- 31 J. Berger, M. Reist, J. M. Mayer, O. Felt, N. A. Peppas and R. Gurny, *Eur. J. Pharm. Biopharm.*, 2004, **57**, 19–34.
- 32 M. J. Moura, H. Faneca, M. P. Lima, M. H. Gil and M. M. Figueiredo, *Biomacromolecules*, 2011, **12**, 3275–3284.
- 33 J. Zhu and R. E. Marchant, *Expert Rev. Med. Devices*, 2011, **8**, 607–626.
- 34 S. Du, N. Zhou, Y. Gao, G. Xie, H. Du, H. Jiang, L. Zhang, J. Tao and J. Zhu, *Nano Res.*, 2020, **13**, 2525–2533.
- 35 L. E. Tracy, R. A. Minasian and E. J. Caterson, *Adv. Wound Care*, 2016, **5**, 119–136.
- 36 R. F. Pereira, C. C. Barrias, P. J. Bártolo and P. L. Granja, *Acta Biomater.*, 2018, **66**, 282–293.
- 37 L. Neufeld and H. Bianco-Peled, *Int. J. Biol. Macromol.*, 2017, **101**, 852–861.
- 38 Y. Yu, H. Yuk, G. A. Parada, Y. Wu, X. Liu, C. S. Nabzdyk, K. Youcef-Toumi, J. Zang and X. Zhao, *Adv. Mater.*, 2019, **31**, 1807101.